Journal of Data Acquisition and Processing
ISSN: 1004-9037
https://sjcjycl.cn/
DOI: 10.5281/zenodo.778025

ENHANCING BRAIN TUMOR DETECTION AND CLASSIFICATION USING A ROBUST HYBRID DEEP TRANSFER LEARNING APPROACH BASED ON MRI DATA

Prasanna Kumar Lakineni [1], Dr. N. Sudhakar Reddy [2], Dr. A. Suresh Babu [3]
[1]Research Scholar, Dept. of CSE, JNTUA College of Engineering Anantapuram, JNTU Anantapur, India
[2]Professor, Dept. of CSE, Sri Venkateswara College of Engineering, Tirupathi, India
[3]Professor, Dept. of CSE, JNTUA College of Engineering Anantapuram, JNTU Anantapur, India

Abstract:
The World Health Organization (WHO) identifies brain tumors as one of the leading causes of death in the world. This disease is challenging to identify because of its complexity and cunning character. Because of the high risk of clinical occurrences, persistent brain tumors illness is a severe public health issue worldwide. Despite the general consensus that persistent brain tumors disease has considerable interactions with elevated risks of vascular events, end-stage excretory organ disease, and all-cause mortality, there is still inadequate information on individuals. Deep learning (DL), a branch of machine learning, has recently shown impressive results, particularly in tasks like classification and segmentation. Imaging can be done in various ways to look for brain tumors. This paper presents a novel solution to a challenging problem through the development of a Deep Hybrid Transfer Learning Based Convolutional Neural Network, referred to as EDTLM. Our proposed approach commences with the preprocessing of MRI images, followed by the design and evaluation of the EDTLM. Through rigorous assessment of loss and accuracy metrics, we sought to enhance the model's performance. To achieve this, we harnessed the power of deep transfer learning by fusing features extracted from these models, thereby significantly improving the classification accuracy for three distinct types of tumors. Our results, obtained from the application of the Hybrid Deep Transfer Learning model, namely the Effinception Deep Transfer Learning Model, underscore the potency of combining deep learning models. This approach not only enhances accuracy in multiclass classification problems but also addresses the challenge of overfitting in the context of imbalanced datasets. Our proposed model aspires to achieve an impressive classification accuracy of up to 99.77%, setting a new benchmark in this domain. Furthermore, our framework consistently demonstrates its competitiveness when juxtaposed with other state-of-the-art studies. This work not only offers innovative insights but also holds great promise for advancing medical image classification tasks.

Keywords: *Brain Tumor, Analysis, Detection, Classification, Hybrid Learning, Ensemble Learning, Transfer Learning, Convolutional Neural Network.*

I. INTRODUCTION:

An abnormal multiplication of brain cells is referred to as a "brain tumors". There are both primary and secondary brain tumors. While secondary tumors begin in several parts of the body, such the skin, lungs, and intestines, before travelling to the brain, primary tumors begin

in the rain. Glioma, pituitary, and meningioma are the three subtypes of tumors based on the cells that give rise to them.

A brain tumors is an abnormal growth of cells within the brain or its surrounding structures. It is a type of tumors that originates in the brain, rather than spreading to the brain from another part of the body (which would be called a metastatic brain tumors). Brain tumors can be benign (non-cancerous) or malignant (cancerous). Benign brain tumors grow slowly and have distinct boundaries, meaning they do not invade nearby tissues. They are generally less life-threatening than malignant tumors and may not require immediate treatment unless they cause significant symptoms or affect important brain functions. Malignant brain tumors, on the other hand, are cancerous and tend to grow more rapidly. They have the potential to invade nearby healthy brain tissue and can expand to other central nervous system regions. Malignant brain tumors can be broken down even further into subcategories depending on the cell type from which they arose, such as gliomas, meningiomas, or metastatic tumors [23,26].

The exact causes of brain tumors are not always known, but certain factors may increase the risk, such as exposure to ionizing radiation, a family history of brain tumors, certain genetic syndromes, and rarely, exposure to certain chemicals or environmental factors. The symptoms of brain tumors can vary depending on their size, location, and rate of growth. Common symptoms include persistent headaches, seizures, changes in vision or hearing, difficulty speaking or comprehending, weakness or paralysis, problems with balance or coordination, and personality or mood changes.

Diagnosis typically involves a combination of imaging tests such as MRI or computed tomography (CT) scans, and in some cases, a biopsy may be performed to obtain a sample of the tumor for further analysis. Figure.1 shows the MRI scans of brain tumors.

The prognosis for a patient with a brain tumors is contingent on many factors, such as the nature of the tumors, its size and location, and the patient's general health. Treatment may involve surgery to remove the tumors, radiation therapy, chemotherapy, targeted drug therapy, or a combination of these approaches [12]. It's important to note that brain tumors can be a complex and serious condition, and treatment outcomes can vary widely depending on individual circumstances. Consulting with a medical professional and a neuro-oncologist is crucial for accurate diagnosis, treatment planning, and ongoing management [18].

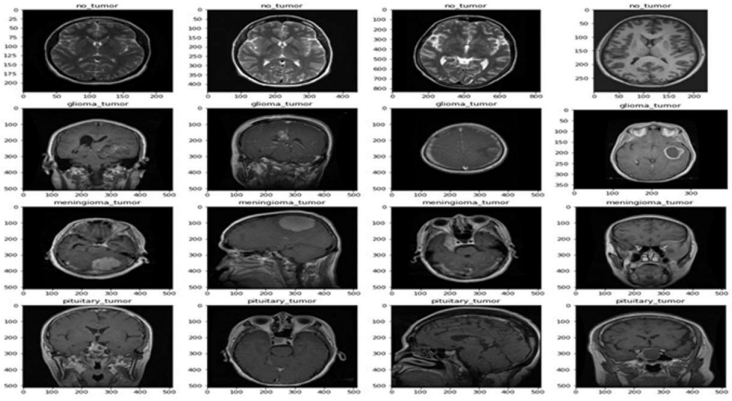

Figure-1. MRI Images of Brain Tumor.

II. Literature Review:

Studies conducted on brain tumors detection and Limitation are presented in the table.1.

Author/Ref.	**Purpose**	**Model**	**Limitations/Future Works**
Gumaei et al. [60]	The purpose of this study is to organize brain tumors using a hybrid feature extraction approach.	RELM	There was no attempt made to compare the approach used in this study with any of the other ML methodologies.
Rehman et al. [83]	In order to categorize brain tumors, we suggest using three different designs of CNNs: alexnet, Googlenet, and vggnet.	CNNs (AlexNet, GoogLeNet, and VGGNet)	Investigate alternative critical DNN topologies that need less time investment for brain tumors classification.
Mittal et al. [67]	In order to diagnose brain tumors using DL-based technologies, the segmentation method is being used.	Combination of SWT and GCNN	It is possible to make use of other databases such as PASCAL, Berkeley, or BRATS. To improve the accuracy of the classifier, it is advised to utilise a number of different classifiers from a range of different domains.
Phaye et al. [23]	Present a strategy for enhancing outputs by employing a network with several deep layers.	DCNet and DCNet++	In order to improve classifier execution, the computational complexity has to be decreased.
Pashaei et al. [78]	Using the CNN and KELM to develop an algorithm for feature extraction and classification.	KELM	Not addressed at all
Abiwinanda et al. [65]	Automatic segmentation and classification of brain tumors may be	CNN	To get more accurate outcomes from classifier, pay close attention to colour balance phase.

	achieved with the help of a CNN.		
Abd-Ellah et al. [56]	Detection of brain tumors by use of an automated detection method with two steps	Classification utilising ECOC-SVM (error-correcting output codes support vector machines), feature extraction employing CNN for preprocessing	Not addressed at all

III. Proposed Methodology:

A hybrid model has proposed as a solution to the early detection and classification of brain tumors in order to fill identified research gaps and accomplish the objectives. Data has collected, cleaned, extract features, classified, and finally evaluated in a series of steps that make up the suggested technique. The first step is data collection; in which we have collect the brain tumors dataset comprised of MRI imaging in preparation for implementation. This dataset is collected from Kaggle website. Next, preprocessing has performed on the images, including resizing to a standard size and applying CLAHE image enhancement techniques to improve the quality and clarity. To reduce noise, a blur method employed. After this normalize the dataset with Minmax normalization by CV2. Then convert images in RGB format, Next, transfer learning models use with two pre-trained models (EfficientNetB7 and Inceptionv3) called Effinception Model. The MRI images are fed into both models, and features extract from intermediate layers of each model. The extracted features are then concatenated to capture a comprehensive representation of the tumor images. Subsequently, a machine learning based XGBoost classifier trained using the concatenated features. The machine learning model optimize by tuning its hyperparameters to enhance its classification performance. The machine learning algorithm that has been trained was tested using relevant assessment measures such as accuracy, precision, recall, and F1 score. When associated to another advanced classification methods for brain tumors, performance of suggested method will be calculated to see whether or not its usefulness can be validated. Overall, the methodology involves data preprocessing, feature extraction using transfer learning, classification using machine learning, hyperparameter optimization, evaluation, and comparison to existing methods to achieve accurate brain tumor classification. The complete system architecture described in this study to identify brain tumors is shown in Fig. 2.

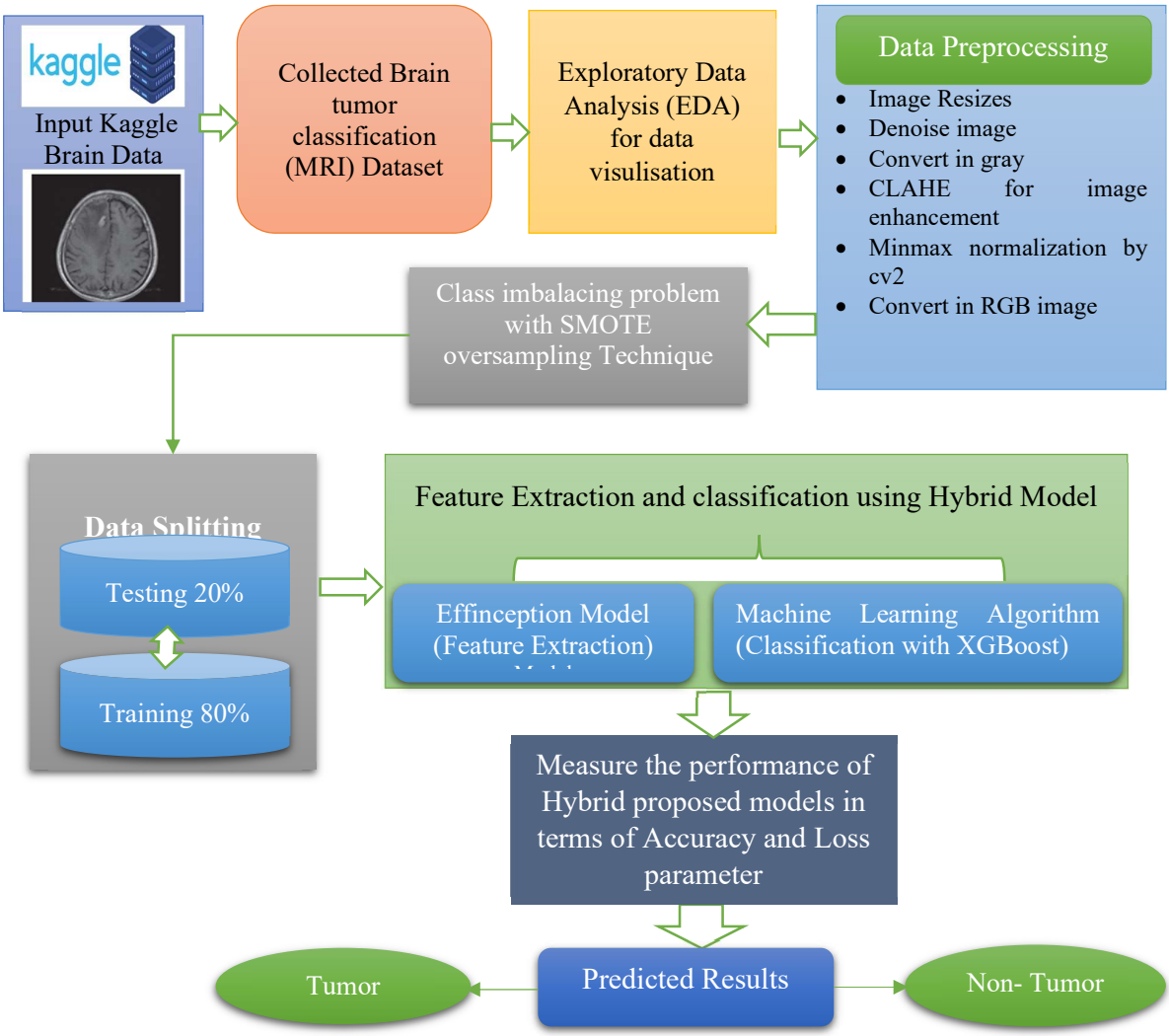

Figure 2: The proposed methodology block diagram

Figure 2 is a flowchart depicting the suggested approach. Gathering patient data is the first step. The next step, following data collection, is data cleaning and preparation. The missing values are completed or eliminated using the procedure outlined in the data preparation section. Various impressive methods were used to enhance the dataset. The cleaned dataset was then split into two smaller datasets: the training dataset and the testing dataset. On the training dataset, the hybrid model was trained using the Effinception and XGBoost method. The suggested approach was evaluated based on its performance on the testing data. The suggested system then generates the outcome once the model has been trained and tested. In technique suggested, patients are classified as either healthy or ill. The implementation of a proposed approach for brain tumor analysis involves the subsequent phases:

IV. Proposed Algorithm:

4.1 Proposed Algorithm-1

Input: MRI imaging dataset
Output: Tumor or Non-Tumor

Step 1: Import MRI imaging Dataset.
Step 2: Carry out operations on the data in order to preprocess the data,

- Converting image RGB
- Resizing image in 98X98
- Used CLAHE image enhancement
- Denoising image
- Minmax normalization by cv2

Step 3: Data Balancing utilising Oversampling approach

- SMOTE stands for Synthetic Minority Oversampling Technique

Step 4: The dataset will be divided into two stages:

- Training_Set (80%)
- Testing_Set (20%)

Step 5: Feature extraction using Transfer learning models

- EffinceptionModel (EfficientNetB7 and Inceptionv3)

Set Parameters:

- Number of Epochs = 180
- Loss function = categorical_crossentropy
- Learning_rate = 0.00001
- Optimizer = Adam ()

Step 6: Classification using machine learning classifier

- XGBoost Classifier

Step 7: Measurement of performance built on both train data as well as test data (Plot the confusion matrix, accuracy graph, or loss graph, as well as precision, recall, as well as F1-score).
Step 8: Lastly, propose on the end result.
End!!!!!!!!!!!!

IV.I Data Collection

In this study, brain tumor dataset[1] have collected that is openly accessible on Kaggle website. The dataset contains a total of 3,060 MRI pictures, which are separated into four categories: 826 images of glioma, 937 photos of meningioma, 396 images of no tumors, and 901 images of pituitary tumors. The size of pixels is consistent throughout all MRI pictures.

IV.II Data Preprocessing

After collecting and loading the dataset, image preprocessing is a necessary initial step in data preparation. It aims to precisely locate objects or areas within images. Data preparation is essential to make computational processes feasible, as real-world data is often incomplete or inconsistent. Data preparation tools enhance data analysis accuracy. Attribute value normalization is a part of this process. There are various data preprocessing methods, including resizing images to a standard size, denoising, converting to grayscale, using CLAHE for enhancement, applying Minmax normalization using cv2, and converting to RGB to improve image quality and clarity.

IV.III Image Resizing

Resizing images means increasing or decreasing their size. Image processing and machine learning both benefit from the ability to scale data. It aids in decreasing an image's pixel count, which has several practical applications. Since the complexity of a model rises in proportion to the number of input nodes, this may speed up the training process for a neural network when an image's pixel count rises. In the research, we resized the image into 98x98 pixels [34].

IV.IV Image Denoising

Denoising is the process of removing unwanted noise or distortions from a signal or data set, often achieved by filtering out noise-causing frequencies. It is used to enhance the efficiency of processing systems. In the fields of Image Processing (IP) and Computer Vision (CV), denoising is applied to clean up noise from magnetic resonance (MR) images. Image denoising utilizes advanced algorithms to significantly improve the quality of images by eliminating unwanted noise. This process aims to clean an image of noise or abnormalities originating from factors like insufficient lighting, low-quality cameras, or compression artifacts. Denoising reduces noise while preserving important features and structures, finding applications in digital photography, medicine, and document processing.

IV.VConvert in Gray

Grayscale conversion is a common image preprocessing technique used in digital photography. It involves removing color information from an image, leaving only shades of grey. In grayscale, each pixel represents the intensity of light, ranging from black (the darkest) to white (the lightest), using values between 0 and 255. This simplifies the image to a black-and-white tonal range, making it the simplest color model.

IV.VI CLAHE for Image Enhancement

Image enhancement is a critical step in various areas of image processing. Images can be degraded by external influences, making it challenging for identification and analysis. Contrast Limited Adaptive Histogram Equalization (CLAHE) is employed to enhance images by reducing distracting elements and highlighting important features, especially in low-light conditions. CLAHE is a method that improves the local characteristics of an image, such as textures and contrast, without excessively amplifying noise. It achieves this through contrast amplification limiting techniques applied to neighboring pixels, resulting in a transformation

function for enhanced image quality and data richness. This process makes images more suitable for research and presentation[45,76].

IV.VII. Minmax normalization by CV2

The first stage in normalisation is to take the MRI image data and average out the extremes of the values for each pixel. This makes the data set as a whole more consistent and equitable, with less potentially misleading noisy information. Database normalisation is a common step in getting data ready for machine learning. To avoid repetition, normalisation adjusts the values of the numerical columns in the dataset to a standard scale without changing the distribution of the values themselves. Normalisation is not necessary for every machine learning dataset. Only when characteristics have varying ranges does it become necessary[3].

Normalization is scaling technique or a mapping technique or a preprocessing stage. Normalization transforms an n-dimensional grayscale image $I = \{X \subseteq R^n\} \rightarrow \{Min, \ldots\ldots, Max\}$ with intensity in the range $I_N: \{X \subseteq R^n\} \rightarrow \{nawMin, \ldots\ldots, nawMax\}$ with intensity values in the range $nawMin, nawMax$. The formula below is used to normalise a digital grayscale picture:

$$I_N = (I - Min)\frac{nawMin - \ nawMax}{Min - \ Max} + newMin \ldots\ldots\ldots\ldots (4.1)$$

If, for instance, image's intensity range is 50 to 180 but the target range is 0 to 255, process would include removing 50 from every pixel's intensity, bringing it down to a range of 0 to 130. After that, intensity of every pixel is multiplied by 255/130, expanding colour space from 0 to 255.

IV.VIIIConvert in RGB image

This process converts your image to RGB - Raw blue, green, and red samples. RGB, that stands for "Red-Green-Blue," is used colour model. This approach, as its name implies, assigns separate numerical values to each of the primaries in order to represent colours. Nearly all modern digital displays use the RGB colour paradigm.

IV.IX. SMOTE for the Data Balancing

The process of modifying the class distribution of a dataset such that each class is shown with an equal or proportionate quantity of data is referred to as "data balancing." The word "data balancing" refers to thi s technique. The dataset has to be balanced in order to improve the accuracy of the forecasting power of the minority class. The Synthetic Minority Oversampling Technique, often known as SMOTE, is a method that is used to address the issue of class imbalance. There are a few different approaches one may use to get a balanced dataset.

IV.X. Synthetic Minority Over-sampling Technique (SMOTE) was proposed by [4] This results in the underrepresented group having fake observations created for them. A given minority class observation and its k nearest neighbours are used to generate a random number that is then used to construct synthetic observations. This procedure is used to each and every observation made of members of a racial or ethnic minority. In SMOTE, the threshold for the number of k-nearest neighbours is set at 5.

V. Exploratory Data Analysis

To put the premise of summary statistics and graphical representations to the test, exploratory data analysis is a step in the research process. It's a strategy for delving into the many forms of information that make up the model. The process univariate visualisation, bivariate visualisation, and multivariate visualisation are only some of the specific statistical functions and procedures that may be carried out using EDA tools. Some of the data visualisation techniques used by the model require the usage of specialised Python libraries including NumPy, Pandas, Keras, SK-Learn, Matplotlib, and Seaborn etc.

V.I. Data Splitting

Following any necessary data cleansing and transformation, the information is partitioned into a training set and a testing set. The Test-Train ratio in this experiment was set to 0.2, meaning that 80% of the images would be utilized to train the proposed model, or 20% would be applied to apply trained neural network and evaluate its validation (test) accuracy.

V.II. Feature Extraction with Transfer learning (Effinception Model)

The classification of a set of features into their respective associated classes is still a difficult task in the field of medical image analysis. The original batch of unprocessed data is sliced and diced into more manageable chunks as part of the dimensionality reduction process, which also includes feature extraction as one of its component steps. Transfer learning, use two models that have already been pre-trained, will be utilised for this procedure. Both models are given the MRI images as input, and the features will be extracted from the intermediate layers of the respective models. After characteristics have been retrieved from the tumors photos, they are concatenated to obtain a full representation of the images.

Next, after preprocessing the data, we will extract the feature. The procedure of feature extraction, which is simply a mixture of the several characteristics that have been extracted in the past, is how new features are produced. The new set of features also includes a system of values, but these values are different from the original feature values. The process of feature extraction may make use of either a big no. of easily computable features or a small no. of very specific traits. Both approaches have their merits. It is essential that the capabilities used in real-world applications can be promptly estimated; hence, the calculations themselves should be lightning-fast and highly effective. Because of this, it is feasible to extract a combination of low and high characteristics from the data. In this study, a feature extract was performed using EfficientNetB7 and Inceptionv3, and the resulting model was given the name **Effinception Model**. The features of both models were integrated, as shown in figure 3.

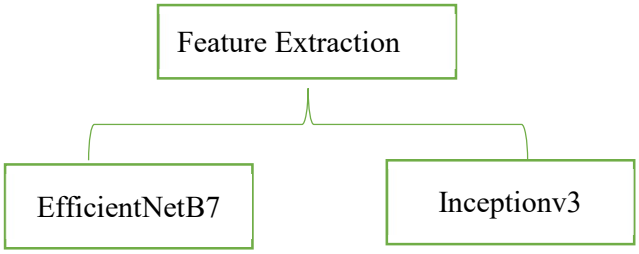

Figure 3: Feature Selection using a deep learning model

EfficientNetB7 as well as Inceptionv3 are the two transfer learning models that are combined to create the hybrid network. For the hybrid model, we are extracting features from both of

these transfer learning models. We've decided to call it the Effinception Model. Deep learning takes use of the transfer learning approach, which employs already existing pretrained models which have been trained on a vast voluminous dataset like as ImageNet. This is done in order to categorize the image without first having to develop the CNN detection algorithms from scratch. ImageNet is one example of such a database. This is done in order to categorize the image. We must improve our model's parameters using transfer learning techniques using Effinception Model-based pretrained hyperparameter models since there are a lot of discrepancies between real pictures and MRI images.

1. EfficientNetB7

EfficientNet [5] is an architecture for a CNN as well as a technique for scaling it that makes use of a compoundcoefficient in order to scale all three dimensions of depth, breadth, and resolution in an equal manner. Utilising what is known as a compound coefficient, Efficientnet is able to efficiently and effectively scale up models in a way that is both simple and sophisticated. In contrast to common practise, which scales various aspects of the network freely, In contrast to the standard procedure, which scales different features of the network without restriction, the Efficientnet scaling approach scales the breadth, depth, and resolution of the network in a consistent way by using a set of specified scaling coefficients. This is in contrast to the standard procedure, which scales various characteristics of the network without restriction. To utilise 2^N times more computer resources, we may enhance network depth by N, network width by N, and image size by N, where constant coefficients are generated by doing a small grid search on the original smaller model. This would allow us to use 2^N times more computational resources. Efficient net makes use of a compound coefficient, which is applied in a reasonable manner, in order to ensure that the breadth, depth, and resolution of the network are all scaled consistently[34,56,12].

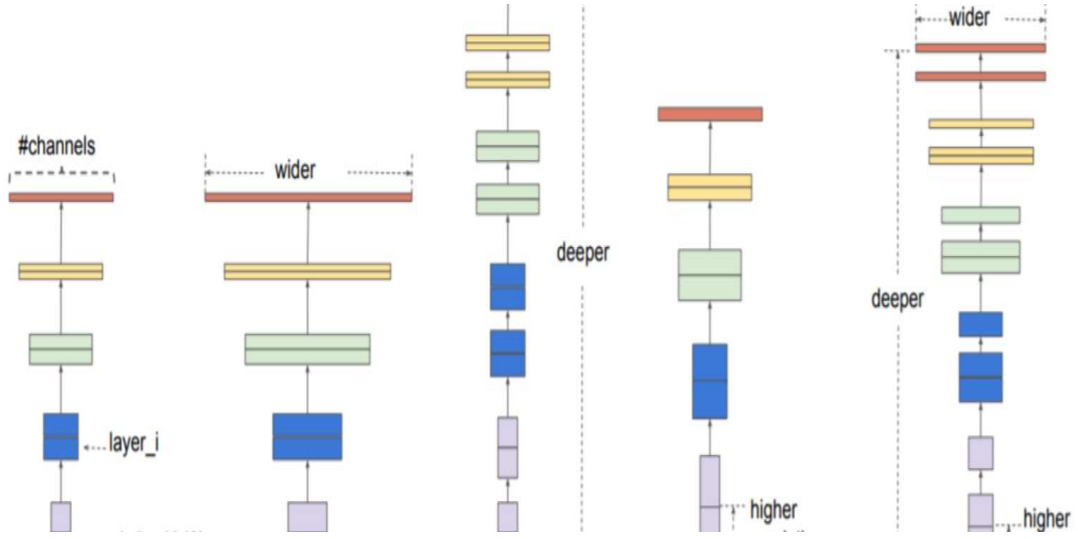

Figure 4: Image classification with EfficientNet Model [6]

The compound scaling technique is supported by the assumption that if input picture is larger, the network will need more layers to extend region of interest as well as channels to catch more fine-grained features on a greater image.

The compound scaling method combines scaling of width, depth, as well as resolution into a single number using a compound coefficient. The formula for scaled characteristics is shown in the next section:

$$\begin{aligned} \text{depth: } & d = \alpha^{\phi} \\ \text{width: } & w = \beta^{\phi} \\ \text{resolution: } & r = \gamma^{\phi} \\ \text{s.t. } & \alpha \cdot \beta^2 \cdot \gamma^2 \approx 2 \\ & \alpha \geq 1, \beta \geq 1, \gamma \geq 1 \end{aligned} \quad \ldots\ldots(4.3)$$

There are three scaling multipliers used here: alpha, beta, as well as gamma. They are resolute by doing a grid search on depth, width, & resolution variables. If, after calculating the preceding equation, we get alpha =1.2, then the new depth is equal to 1.2 * the previous depth.[32]

ø is a user-specific co-efficient that accepts real values such as that controls resources, where 2ø is the number of resources. To put it another way, if we have twice the resources available than what a model is presently using, we may find by using 2ø = 2, and therefore ø is 1 in such situations.

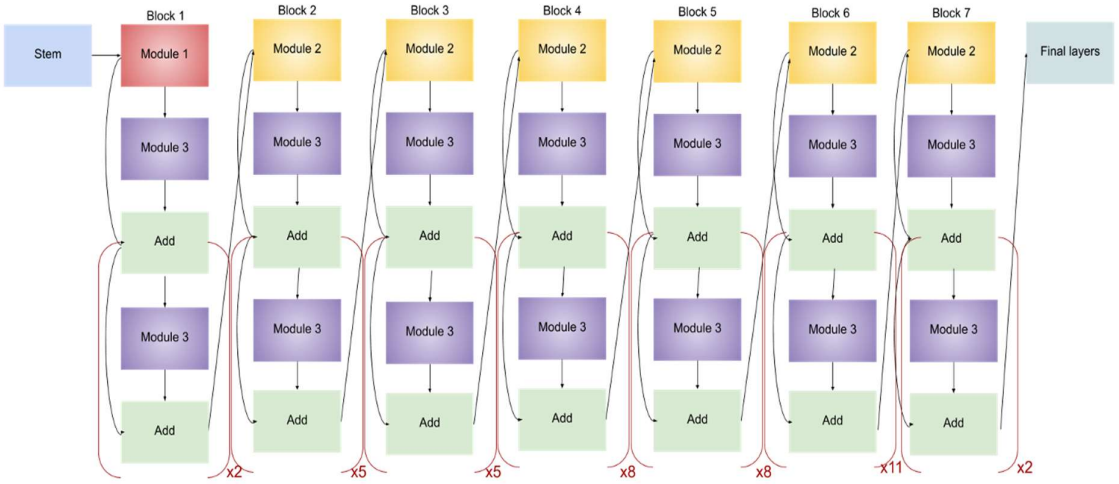

Figure 5: Architecture of EfficientNet-B7

Convolutional neural networks are available in several configurations, each with its own set of advantages. These models have shown outstanding performance in varied range of computer vision applications, even though their designs differ. EfficientNet is one of these CNN variations that has been developed. The Efficientnet-B7 model is EfficientNet models intended to complete image classification. In EfficientNet-B7, the total amounts to 813 points. However, all of these levels may be constructed from the five modules indicated below.

- **Module 1:** The future sub-blocks will build off of this as their starting point.

- **Module 2:** Despite the exception of the first major block, this serves as the starting point for first sub-block of each of the next seven major blocks.
- **Module 3:** From this point on, there will be skip links to each and every one of the sub-blocks.
- **Module 4:** This is what is used to link the first sub-blocks to one another when the skip connection is used in those initial sub-blocks.
- **Module 5:** In the form of a skip connection, each sub-block is connected to the one that came before it, and in actuality, the sub-blocks are merged with the assistance of this module.

2. Inceptionv3

Inception In 2014, the Google Brain Team launched and created a CNN network under the moniker GoogleNet. This network was trained using the ImageNet database. Inception was a network that had been pretrained with 22 layers and 5M parameters. It had a kernel (filter) dimension of 1 1, 3 3, and 5 5 to collect handmade information at varying sizes. One of those levels was the max-pooling layer. The usage of filters with 1 x 1 kernels is recommended for the purpose of preserving computation time while having a less influence on the performance of the network. In the latter half of 2015, Google upgraded their Inception network to the Inception-v3 variant, which has convolutional layers that have been downscaled using hyperparameters. Inception-v3 is a deep neural network that has 48 layers and was designed to classify MRI brain pictures into one thousand different image classes while also avoiding overfitting issues. (e model has the power of self-learning to extract multiple handmade characteristics from photos and analyse them for brain image categorization. The Inception-v3 network needs an input picture that is 299 pixels wide and 299 pixels tall. Batch normalisation, RMSprop, and picture distortion are some of the techniques that Inceptionv3 use to achieve improved performance in computer vision challenges. The fundamental structure of the Inceptionv3 model is shown here in figure 6. [7].

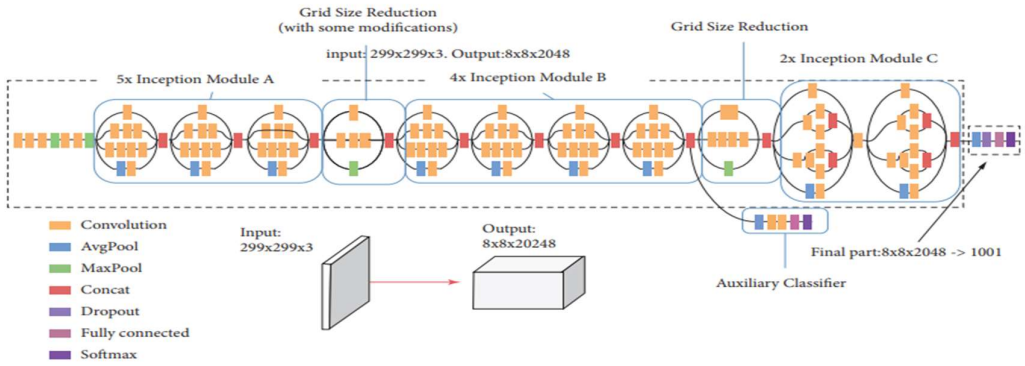

Figure 6: Inceptionv3 model [7]

The convolutional neural network known as Inceptionv3 was initially designed to function as a module for Googlenet. The major objective of this tool is to provide assistance with the processes of image processing as well as object recognition. It is 3rd version of Google's Inception CNN, that was first shown at the ImageNet Recognition Challenge. This particular challenge was held to test the capabilities of neural networks to recognize images. It was proposed that the Inception-V3 pre-trained models be employed in this situation [8]. This

model, which consists of more than 20 million parameters, was trained by one of the most accomplished hardware experts the industry has to offer. The algorithm itself is composed of symmetrical including asymmetrical components that include various convolutional, average as well as max pooling, concats, dropouts, and FCLs. These building blocks may be arranged in either a symmetrical or an asymmetrical pattern. In addition to that, the input from the activation layer into this model is often subjected to batch normalization processing.

3. Model hyper parameter

The Effinception Model hyperparameters are given below

1) Loss Function

The loss function is an important topic in deep learning since it reveals how well the model fits the data. When a model's loss function is less, it means that the model is doing a better job of fitting the data. It is also expected that when the loss function is high, the corresponding gradients will be large enough to provide a faster update as gradient decreases [45]. Also, loss function is quite significant during model training. The best network parameter training technique may be obtained by the training method's guidance by backpropagating the errors introduced through the use of anticipated sampling in addition to the real sample labels.

Categorical_Crossentropy: This is a loss function that is used in work that involves the categorization of several classes. If the model is presented with a task that indicates an instance may only be placed into one of a number of possible categories, it is responsible for determining that category the instance belongs to. In multi-class classification models, in which there are two or more output labels, this function has been employed as a loss function. A string of zeros and ones is what is allocated to the output label, and this string is used to represent the value of a single category encoding. For the purpose of categorical classification, the "negative log-likelihood (NLL)" is equivalent to the "cross-entropy loss" that is brought about by the training data point $\boldsymbol{i}_{,}(\boldsymbol{x_i}, \boldsymbol{y_i})$:[48]

$$L_i = -\log\left(p_{y_i}\right) \dots\dots\dots\dots\dots (1)$$

given that the chance of $\boldsymbol{y_i}$being right is one and that of all other labels is zero, ground truth probability is one.

2) Adam Optimizer (Adaptive Moment Estimation)

Adam is an adaptive learning system that strives to increase performance by using rate optimisation. Whenever any of the variables are altered, this ensures that element-wise moving average of squared values and parameter gradients remain unaltered. Additionally, it contributes a momentum component to the equation and maintains their integrity.

Adam is another adaptive learning algorithm with rate optimization similar to RMSProp. It adds a momentum term when the parameters are updated and retain the element-wise moving average of the squared values and the parameter gradients [9],

$$m_\epsilon = \beta_1 m_{\epsilon-1} + (1-\beta_1)\nabla E(\theta_\epsilon)$$

$$v_\epsilon = \beta_2 v_{\epsilon-1} + (1-\beta_2)[\nabla E(\theta_\epsilon)]^2 \quad \dots\dots.(2)$$

Adam updates the network parameters by employing the moving averages as

$$\theta_{\ell+1} = \theta_{\ell} - \frac{\alpha m_l}{\sqrt{v_l} + \epsilon} \quad \text{.....(3)}$$

where ε >0 is a small constant and is added to avoid division by zero. We see from the expression that the calculation of the updated step size can be adaptively adjusted from the two angles of gradient mean and gradient square, instead of being directly determined by the current gradient.

3) Effect of Batch Size

Batch size defines the number of input samples that are passed on to the network. Batch size is also an influencing parameter which determines the accuracy of classification. Larger the batch size, more time it takes for the training of dataset, and eventually the accuracy of the model decreases and also affects the memory requirement. So, we should be very careful when choosing the batch size. This model is executed with the following batch sizes: 8,16,32,64. The model's accuracy is increased when there is an increase in the batch size from 8 to 16, slightly decreased at 32, and decreased at a batch size of 64. It is observed that at batch size 64, the Effinception Model produced the highest accuracy[34].

4) Effect of optimizers

Optimizers are used in optimizing the performance of our model by updating weight parameters which minimize our loss function. Our objective is to reduce the loss of our neural network by enhancing the parameters of our network. The loss function calculates loss by matching the true value and predicted value by a neural network. Here in our work Effinception Model, we evaluated Adam optimizer is the best optimizer for our model giving the accuracy[56].

5) Effect of learning rates

During the training of the neural network, some amount of weights is updated. These weights are called learning rates. This is an important hyperparameter used in the CNN model whose range is between 0.0 and 1.0. In our model, we adopted four learning rates and observed the effects of those learning rates on accuracy. The four learning rates are 0.1, 0.01, 0.001, and 0.0001. Here we used 0.00001 best learning rate of Effinception Model[76].

6) Effect of Number of epochs

Epochs are nothing but the number of iterations. Now by keeping the batch size constant at 3 64, learning rate at 0.00001 and using Adam optimizer the model is trained at epochs:180 of Effinception Model [44].

4. XGBoost Regressor (Extreme Gradient Boosting) Classifier

We employed the XGBoost machine learning classifier for brain tumor prediction and classification. XGBoost uses boosting, a method that combines weaker classifiers into a strong classifier. It adds new classifiers during training, and in XGBoost, decision trees act as weak classifiers. This algorithm effectively addresses structured data challenges through gradient boosted trees during learning. XGBoost optimizes a formalized objective function by considering the difference between observed and target outputs, incorporating computing

complexity. The training process is iterative, with additional trees predicting residuals and improving overall predictions. Equations below show this hallmark.

$$F_0 = 0 \dots \dots \dots (5)$$

$$F_t = F_{t-1}(x) + h(x) \dots \dots \dots (6)$$

There, the decision tree that results from $F_{t-1}(x)$ is denoted by h(x), while the entire model that results from t-1 steps is denoted by $F_t(x)$) The goal of the XGBoost model is to locate the tree that, at the t-1 step, has the equation (7) minimized to the greatest extent possible t^{th} step.

$$Obj(F_t) = L(F_{t-1} + F_t) + \Omega(F_t) \dots \dots \dots (7)$$

In this context, L stands for the loss function that determines the predictive capacity, and Ω is represents the regularization function that keeps overfitting in check. The structure of XGBoost is shown in Figure. 7

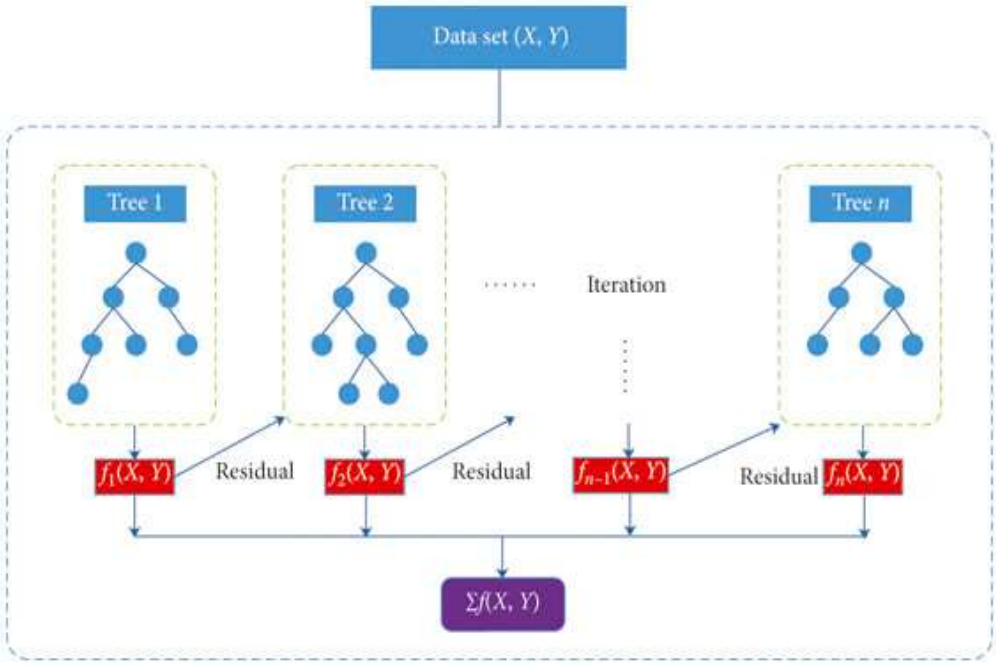

Figure 7: Structure of XGBoost

XGBoost supports parallelization by creating decision trees in a parallel fashion. Distributed computing is another major property held by this algorithm as it can evaluate any large and complex model. It is an out-core-computation as it analyses huge and varied datasets. Handling of utilization of resources is done quite well by this calculative model. An extra model needs to be implemented at each step-in order to reduce the error.

XGBoost objective function at iteration t is[17]:

$$L(t) = \sum_{i=1}^{n} L(y\_out_i, y\_out1_i^{(t-1)} + f_t(x_i) + g(f_t) \quad \dots\dots\dots(4.11)$$

where, y_out = real value know from the training dataset, and the summation part could be said as f(x + dx) where x= $y\_out1_i^{(t-1)}$).

V.III. Dataset Description

In this study, we used the "Brain Tumour Classification (MRI)" dataset, which contains four distinct tumor classes: glioma, meningioma, pituitary tumors, and no tumors. Brain tumors are highly dangerous, with the majority of primary central nervous system tumors originating in the brain. Each year, around 11,700 new cases of brain tumors are diagnosed in the United States. Survival rates vary, with a 34% chance of surviving five years for those with cancerous brain or nervous system tumors, slightly higher for women.

Various brain tumor types, including benign and malignant tumors, belong to the same category. Accurate diagnosis and treatment are critical for extending life expectancy. Magnetic Resonance Imaging (MRI) is the most effective diagnostic tool for brain tumors, generating substantial image data. Radiologists use these images for diagnosis due to the intricacy of brain tumors. The dataset includes 3,060 MRI images divided into four groups: 937 meningiomas, 826 gliomas, 396 tumors, and 901 pituitary tumors. The MRI images have a resolution of 512 pixels on each side.

After preprocessing, the images are categorized into Training and Testing folders. Each folder contains subfolders with MRI scans of different tumor types. The study applied normalization, enhancement, image conversion, and grayscale conversion to the images from the dataset.

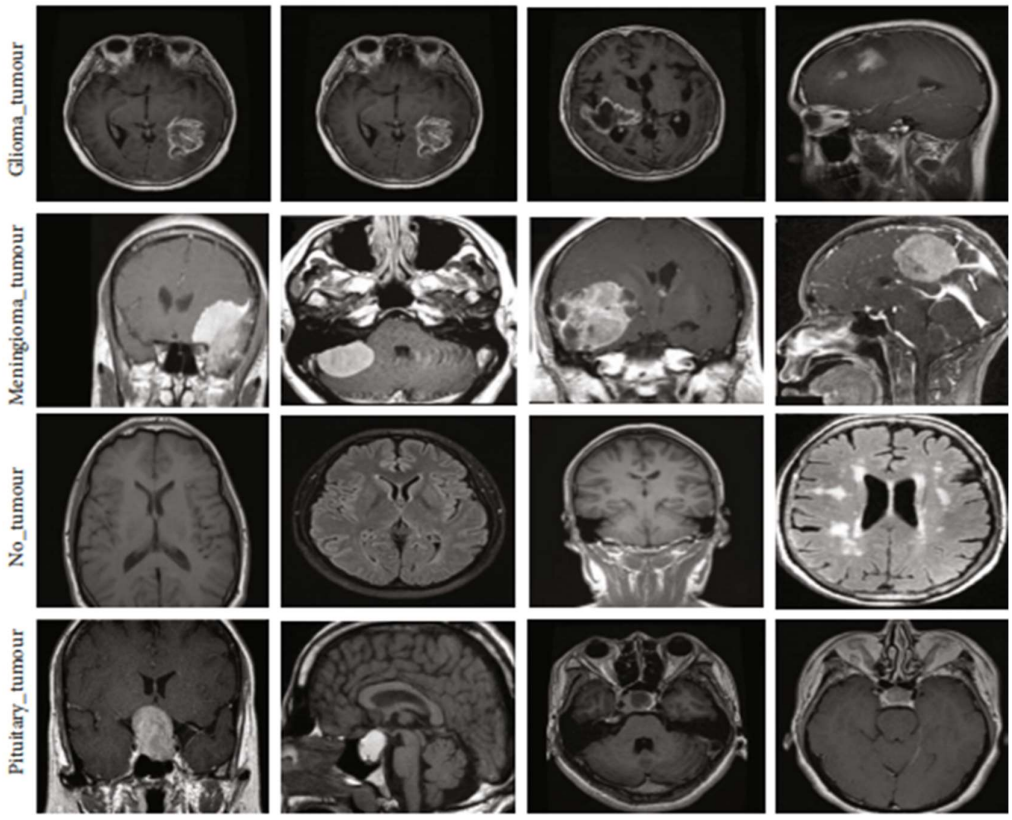

Figure 8: Samples of a dataset of an MRI of brain tumors.

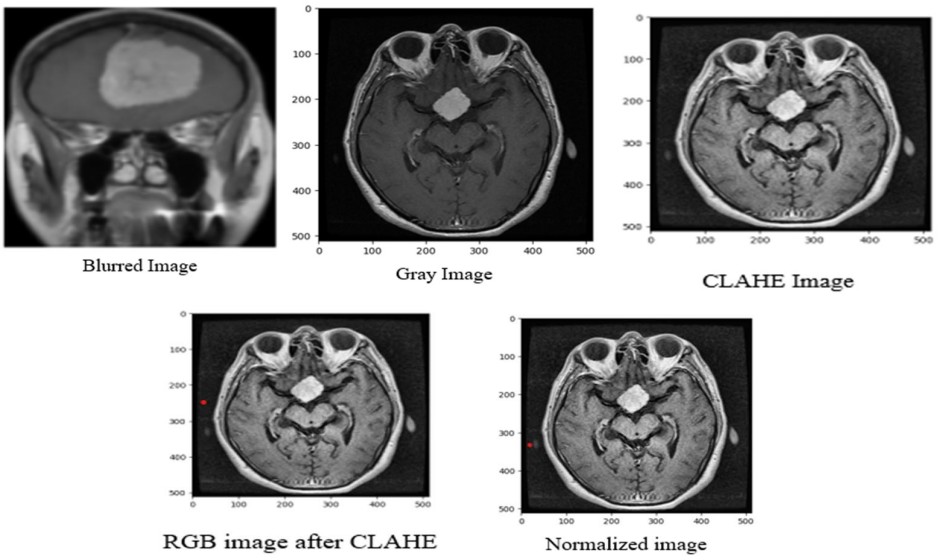

Figure 9: samples from a dataset after preprocessing.

VII. Performance Measurements

To assess our model's accuracy, we need to discuss the performance metrics. These metrics rely on the provided labels in the database and are essential for evaluating the model. We evaluate the model's performance by testing it with a set of examples and tracking the number of errors it makes.

VII.I. Confusion Matrix (CM)

1. Accuracy(acc)

$$\text{Accuracy} = \frac{\text{True Positive} + \text{True Negative}}{\text{True Positive} + \text{True Negative} + \text{False Negative} + \text{False Positive}} \ldots\ldots (5.1)$$

2. Precision(pre)

$$\text{Precision} = \frac{\text{True Positive}}{\text{True Positive} + \text{False Positive}} \ldots\ldots (5.2)$$

3. Recall or (Sensitivity) (rec)

$$\text{Recall} = \frac{\text{True Positive}}{\text{True Psitive} + \text{False Negative}} \ldots\ldots (5.3)$$

4. F1-Score (F1)

$$F1 = 2 * \frac{\text{precision} \cdot \text{recall}}{\text{precision} + \text{recall}} \ldots\ldots (5.4)$$

5. True Positive Rate (TPR)

$$\text{TPR} = \frac{\text{True Positive}}{\text{True Psitive} + \text{False Negative}} \ldots\ldots (5.5)$$

6. False Positive Rate (FPR)

$$\text{FPR} = \frac{\text{False Positive}}{\text{False Positive} + \text{True Negative}} \ldots\ldots (5.6)$$

7. Area under the Curve

The size of empty area that is below ROC curve looks like this. ROC is a graph in that TPR is displayed along the y axis and FPR is plotted along x axis for variety of thresholds. AUC is a useful metric for measuring effectiveness of ML models. The quality of ML model improves in proportion to increase in AUC.

$$AUC = \int_0^1 \frac{TP}{TP+FN} d \frac{FP}{TN+FP} \quad \text{.....(5.7)}$$

8. Receiver operating characteristics (ROC)

It is a representation of a trade-off between two criteria, including and specificity, & sensitivity on plane that the two measurements cover. Research in the field of biomedical informatics typically makes use of ROC curves in order to assess categorization and models of prediction for the purposes of decision assistance, diagnosis, and prognosis. In addition, ROC curves are used in the process of evaluating the correctness of framework as well as its capacity to differentiate between positive and negative scenarios.

VIII. Simulation Results of Proposed Model

1. Proposed Effinception Model Results

In this section provide simulation outcomes of Effinception Model. For hybrid model we are extracting features from two transfer learning model by concating two transfer learning model which is Efficientet B7 and Inception v3. we name it as Effinception Model. We use this model for both feature extraction and also for classification. Her we provide the implemented results of this model in form of graphical representation.

Table 2: Test and Train performance of proposed Transfer Learning based Effinception Model

Train Accuracy	Train Loss	Test Accuracy	Test Loss
99.87	0.0145	91.87	0.2985

The above table 2 test and train performance of proposed Transfer Learning based Effinception Model in terms of loss or acc. The proposed Effinception Model train and test accuracy 99.87% and 91.87% while train or test loss 0.0145 and 0.2985% respectively.

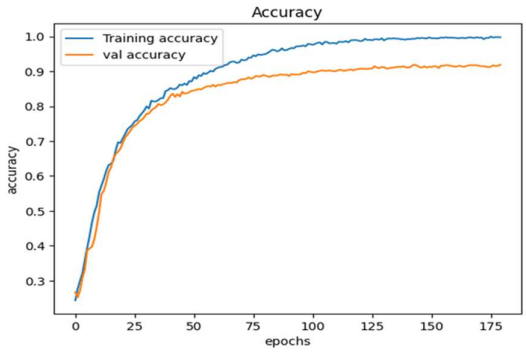

Figure 10. Plot graph of training and validation accuracy vs epochs using Transfer Learning based Effinception Model

The above fig 10shows train and val accuracy vs epochs using TL based Effinception Model using 0 to 180 number of epochs. One example of a hyperparameter is no. of epochs. It determines how many times the learning algorithm must process the complete dataset. Accuracy during training and validation are plotted against time in the figure, which is represented by the x axis. Both the blue and orange lines on the graph represent accurate results. During validation, a model's accuracy is measured by how well it does on data it has never seen before. During training, a model's accuracy is measured by how well it does on the data it was trained on. Due to the model's unfamiliarity with the validation data, training accuracy tends to be higher. The proposed Transfer Learning based Effinception Model shows 99% accuracy with brain tumor dataset and validation accuracy is 91% respectively.

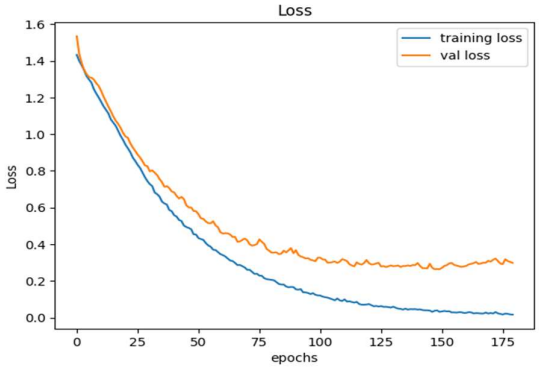

Figure 10 : Plot graph of training and validation loss vs epochs using TL based Effinception Model

Figure 10 illustrates the train as well as val loss vs the number of epochs for an Effinception Model that is based on TL and uses anywhere from 0 to 180 epochs. The figure's y-axis displays numbers for training and validation loss while the x-axis displays the number of epochs. The capacity of the model to fit new information is shown by both training loss & validation loss. The training loss metric provides insight into the degree of alignment between model and training data. The proposed EffinceptionModel shows 0.0145% loss with brain tumor dataset and validation loss is 0.2985% respectively.

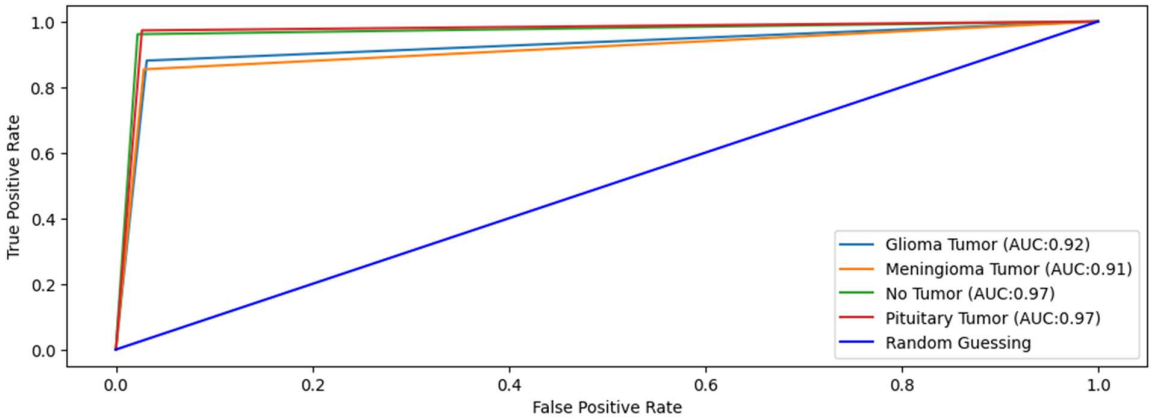

Figure 11: ROC curve of multiclass classification using brain tumor dataset using Transfer Learning based Effinception Model

The above figure 11. shows the ROC curve of multiclass classification using brain tumor MRI dataset using Transfer Learning based Effinception Model, The MRI dataset contain four classes that already described section 5.1 in dataset description. The true positive rate, also called as TPR, is shown on y axis of a ROC curve, while false positive rate, also called as FPR, is plotted on the x axis. Because of this, the point in upper left corner of plot that has an FPR of zero and a TPR of one is considered to be "ideal" location. Even though this is impractical, it indicates which a larger AUC (area under the curve) is frequently preferred. It is desired to optimize TPR while minimizing FPR; consequently, "steepness" of ROC curves should be considered. After binarizing the result, one may acquire a concept of TPR or FPR when dealing with multiclass classification. The first-class glioma tumor AUC is 92%, second class meningioma tumor class AUC is 91%, class third no tumor is AUC 97% while pituitary tumor AUC is 97% respectively.

	precision	recall	f1-score	support
Glioma Tumor	0.90	0.88	0.89	176
Meningioma Tumor	0.91	0.85	0.88	185
No Tumor	0.94	0.96	0.95	206
Pituitary Tumor	0.92	0.97	0.95	183
accuracy			0.92	750
macro avg	0.92	0.92	0.92	750
weighted avg	0.92	0.92	0.92	750

Figure 12: Classification report of proposed using Transfer Learning based Effinception Model
The above figure 12 demonstrations classification report of suggested Effinception Model using brain tumor MRI images that contain four classes. The first-class glioma tumor precision is 90%, 88% recall, 89% f1-score with support 176, second class meningioma tumor class precision is 91%, recall 85%, f1-score 88% with support 185, class third no tumor is precision is 94%, recall 96%, f1-score 95% with support 206, while pituitary tumor precision is 92%, recall 96%, f1-score 95% with support 183. The whole accuracy of proposed model is 92% with support 750 respectively.

```
Training Accuracy : 0.9987
Validation Accuracy : 0.9187
Precision : 0.9182
Recall : 0.9187
f1 score : 0.9180
```

Figure 13: Parameter performance of Transfer Learning based Effinception Model
The above figure 5.7 shows the parameter performance results of Transfer Learning based Effinception Model using brain tumor MRI image dataset. This model obtains train accuracy 99%, validation accuracy 91% while precision, recall and f1-score is also 91% respectively.

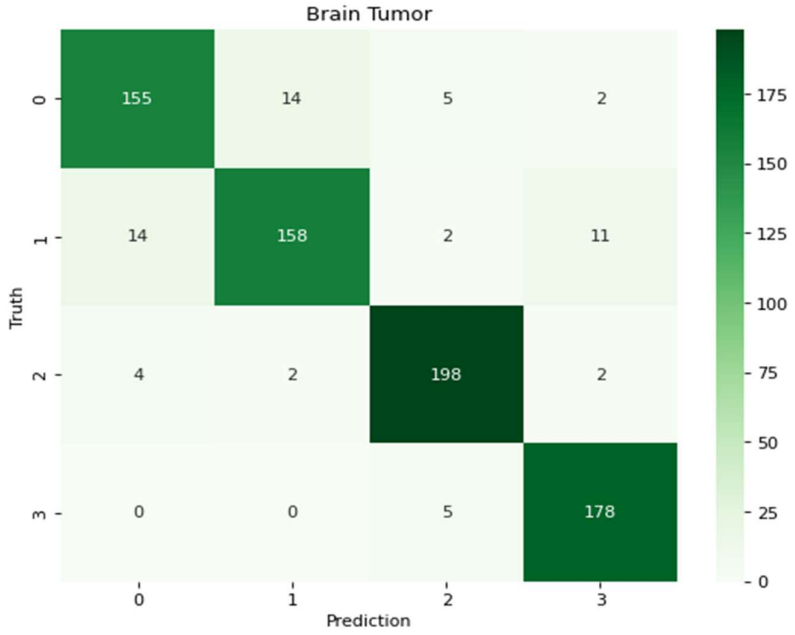

Figure 13: Confusion Metrix of proposed using Transfer Learning based Effinception Model

The above figure 5.8 shows the Confusion Metrix of multiclass classification using brain tumor MRI dataset using Transfer Learning based Effinception Model, The MRI dataset contain four classes, where first-class (0) glioma tumor total predicted images is 155%, second-class (1) meningioma tumor class total predicted images is 158%, class-third (3) no tumor is total predicted images 198% while class-four (4) pituitary tumor total predicted images is 178 respectively.

9. Proposed XGBoost Model Results

In this section provide simulation results of ML based XGBoost classifier. We use ML based XGBoost classifier for classification. Her we provide implemented results of this model in form of graphical representation.

	precision	recall	f1-score	support
Glioma Tumor	0.97	0.84	0.90	176
Meningioma Tumor	0.87	0.91	0.89	185
No Tumor	0.95	0.97	0.96	206
Pituitary Tumor	0.92	0.97	0.95	183
accuracy			0.93	750
macro avg	0.93	0.92	0.92	750
weighted avg	0.93	0.93	0.92	750

Figure 14: Classification report of proposed using Machine Learning based XGBoost Classifier

The above figure 14 demonstrations classification report of proposed XGBoost model using brain tumor MRI images that contain four classes. The first-class glioma tumor precision is 97%, 84% recall, 90% f1-score with support 176, second class meningioma tumor class precision is 87%, recall 8591 f1-score 89% with support 185, class third no tumor is precision is 95%, recall 97%, f1-score 96% with support 206, while pituitary tumor precision is 92%,

recall 97%, f1-score 96% with support 183. The complete accuracy of proposed XGBoost Classifer is 94% with support 750 respectively.

```
Precision : 0.9272
Recall : 0.9253
f1 score : 0.9249
```

Figure 15: Parameter performance of Machine Learning based XGBoost classifier

The above figure 15 shows the parameter performance results of XGBoost classifier using brain tumor MRI image dataset. This model obtains pre, rec and f1 is 92% respectively.

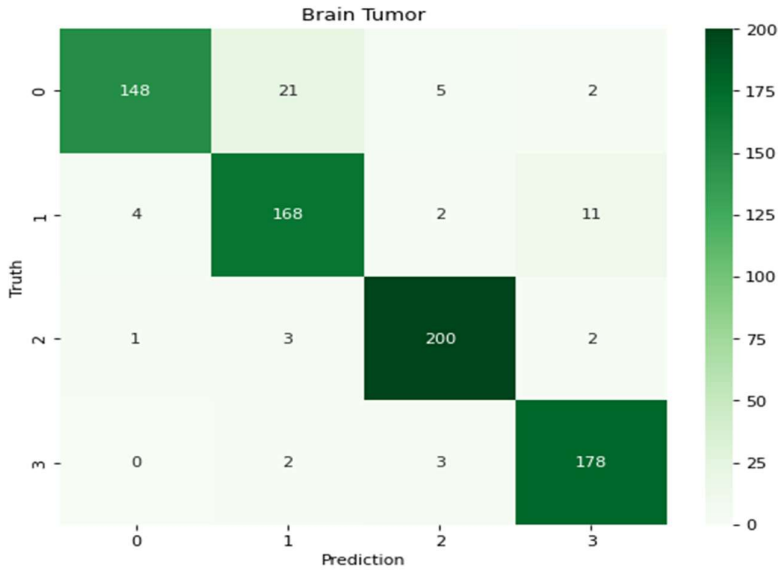

Figure 16: Confusion Metrix of multiclass using Machine Learning based XGBoost classifier, The above figure 516 shows the Confusion Metrix of multiclass classification using brain tumor MRI dataset using XGBoost Model, The MRI dataset contain four classes, where first-class (0) glioma tumor total predicted images is 148, second-class (1) meningioma tumor class total predicted images is 168, class-third (3) no tumor is total predicted images 200 while class-four (4) pituitary tumor total predicted images is 178 respectively.

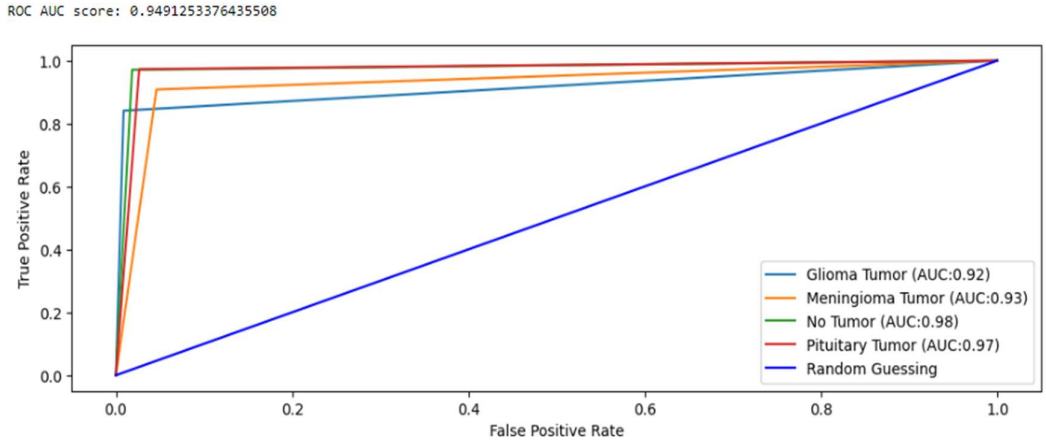

Figure 17: ROC curve of multiclass classification using brain tumor dataset using Machine Learning based XGBoost classifier

The above fig 17 shows WROC curve of multiclass classification using brain tumor MRI dataset using XGBoost Model, The MRI dataset contain four classes the first-class glioma tumor AUC is 92%, second class meningioma tumor class AUC is 93%, class third no tumor is AUC 98% while pituitary tumor AUC is 97% also overall ROC-AUC score of proposed XGBoost classifier is 94% respectively.

VIII. Comparative Analysis

This section offerings the comparative analysis between proposed and previous models. As presented above about the proposed results in which Effiinception model is proposed in this work. Below, we have contrasted performance outcomes of Effiinception model with previous models on same dataset.

Table 5.3: Test and Train performance of proposed Transfer Learning based Effinception Model

Models	**Train Accuracy**	**Test Accuracy**	**Precision**	**Recall**	**F1-Score**
Effinception+XGBoost	99.87	91.87	91.82	91.87	91.80
EfficientNet+XGBoost	94.13	84.27	85.50	84.27	83.90
Inception+XGBoost	91.69	86.27	88.24	86.27	86.60

In the table below, we compare the results of three popular machine learning models: Effinception, EfficientNet, and Inception. The table below compares the suggested Effinception model to many alternative models. A dataset was utilized to test & train these models. Effinception had the greatest accuracy (99.87%) on the training data, followed by EfficientNet (94.13%) and Inception (91.69%) in the "TrainAccuracy" column. As can be seen in the "TestAccuracy" column, Effinception retains the best accuracy (91.87 percent) when applying the model to new data, whereas EfficientNet and Inception have lesser accuracies (84.27 percent and 86.2 percent, respectively). Positive class prediction accuracy, true positive capture rate, and harmonic mean are all measures of model quality that can be accessed through the "Precision," "Recall," and "F1-Score" metrics. When it comes to accuracy, recall, and F1-Score, Effinception once again demonstrates superior performance compared to its rivals. In conclusion, Effinception demonstrates the best performance across all categories, following in decreasing order of performance by EfficientNet and Inception.

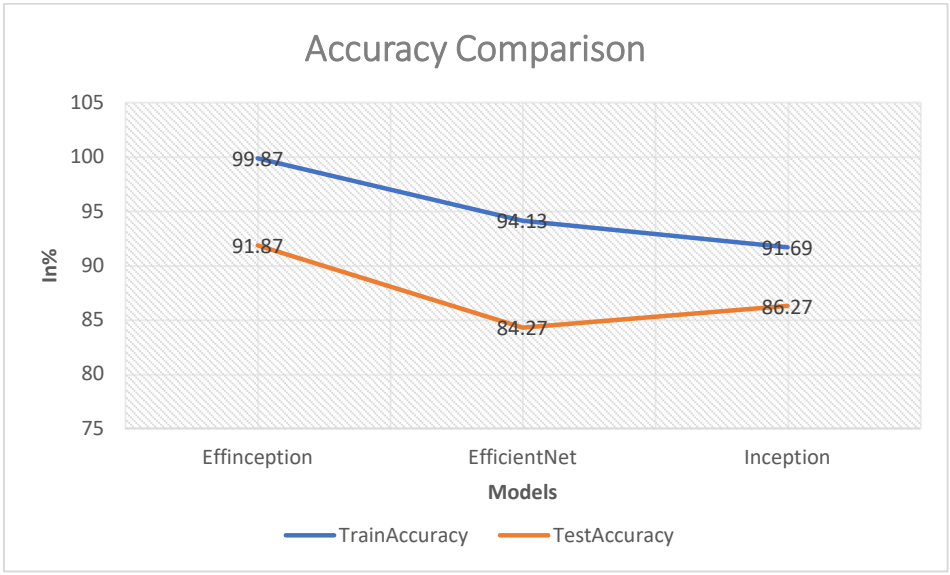

Figure 18: Accuracy Comparison

The above figure 5.13 shows a line graph which compares the proposed model accuracy with previous models. In this figure, x-axis represents various models, & y-axis represents accuracy values in percentage. The training accuracy of proposed Effinception model is 99.87percent, 94.13percent for EfficientNet and 91.69percent for Inception model, whereas the testing accuracy of each model is 91.87% for Effinception, 84.27% for EfficientNet, and 86.27% for Inception, respectively.

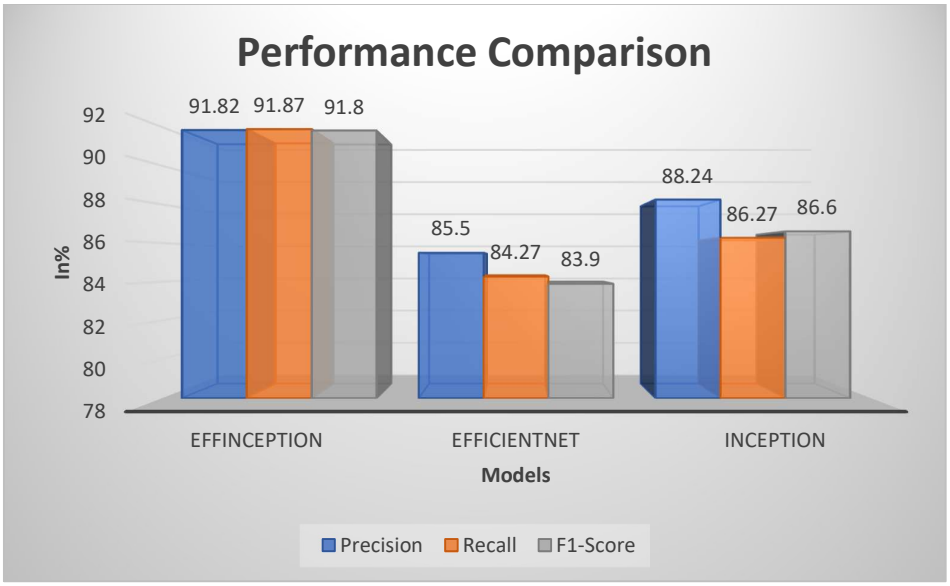

Figure 19: Performance Comparison Between Proposed and Existing Models

Figure 5.14 presents a bar graph that compares the performance of suggested and current models in terms of recall, precision, and f1-score performance measures. The x-axis represents the different model such as Effinception, EfficientNet, and Inception, and y-axis represents the performance values in percentage. The obtained highest performance results are 91.82% of precision, 91.87% of recall, 91.80% of f1-score for proposed Effinception model, 85.50% of

precision, 84.27% of recall, 83.90% of f1-score for EfficientNet model, and 88.24% of precision, 86.27% of recall, 86.60% of f1-score for Inception model, respectively.

IX: Conclusion:

An efficient brain tumor diagnosis system is necessary for the early treatment of the patient. In this regard, a new two-phase brain tumor detection and classification framework is proposed to improve brain tumor diagnosis and reduce computational complexity. In the detection phase, we proposed a novel Effinception Model for differentiating brain tumor instances from normal individuals with fewer false negatives, and performance is compared with the existing DL techniques. Experimental results demonstrate that the proposed Effinception Model outperformed by achieving an accuracy (99.87 %), Recall (91.87), Precision (91.82), F1-Score (91.80). The simulation analysis reveals that the recommended strategy gives superior results when contrasted to procedures that are currently considered to be state-of-the-art. Using results thus obtained a hybrid EffinceptionModel and XGBoost classifier model has been built to get better accuracy and prediction results. This contributes to growth of MLs for the early diagnosis of brain cancer and assists medical professionals in more precisely identifying patients. This is based on the improved performance of the hybrid approach that has been suggested. two-phase framework is expected to assist clinicians in decision-making in clinical practice and will be helpful for radiologists in brain tumors diagnosis. In the future, we will appraise our proposed framework's performance and a more optimized one on other medical image datasets.

REFERENCES:

[1] M. J. Lakshmi and S. N. Rao, ‘‘Brain tumor magnetic resonance image classification: A deep learning approach,’’ Soft Comput., vol. 26, no. 13, pp. 6245–6253, Jul. 2022, doi: 10.1007/s00500-022-07163-z.

[2] W. Jun and Z. Liyuan, ‘‘Brain tumor classification based on attention guided deep learning model,’’ Int. J. Comput. Intell. Syst., vol. 15, no. 1, p. 35, Dec. 2022, doi: 10.1007/s44196-022-00090-9.

[3] A. Rehman, S. Naz, M. I. Razzak, F. Akram, and M. Imran, ‘‘A deep learning-based framework for automatic brain tumors classification using transfer learning,’’ Circuits, Syst., Signal Process., vol. 39, no. 2, pp. 757–775, Feb. 2020, doi: 10.1007/s00034-019-01246-3.

[4] T. Fernando, H. Gammulle, S. Denman, S. Sridharan, and C. Fookes, ‘‘Deep learning for medical anomaly detection—A survey,’’ ACM Comput. Surveys, vol. 54, no. 7, pp. 1–37, Sep. 2022, doi: 10.1145/3464423.

[5] A. S. Lundervold and A. Lundervold, ‘‘An overview of deep learning in medical imaging focusing on MRI,’’ Zeitschrift für Medizinische Physik, vol. 29, no. 2, pp. 102–127, 2019, doi: 10.1016/j.zemedi.2018.11.002.

[6] L. Rundo, C. Militello, S. Vitabile, G. Russo, P. Pisciotta, F. Marletta, M. Ippolito, C. D’Arrigo, M. Midiri, and M. C. Gilardi, ‘‘Semi-automatic brain lesion segmentation in gamma knife treatments using an unsupervised fuzzy C-means clustering technique,’’ in Advances in Neural Networks (Smart Innovation, Systems and Technologies), vol. 54. Cham, Switzerland: Springer, 2016, doi: 10.1007/978-3-319-33747-0_2.

[7] S. Bonte, I. Goethals, and R. Van Holen, ‘‘Machine learning based brain tumour segmentation on limited data using local texture and abnormality,’’ Comput. Biol. Med., vol. 98, pp. 39–47, Jul. 2018, doi: 10.1016/j.compbiomed.2018.05.005.
[8] C. Militello, L. Rundo, S. Vitabile, G. Russo, P. Pisciotta, F. Marletta, M. Ippolito, C. D’arrigo, M. Midiri, and M. C. Gilardi, ‘‘Gamma Knife treatment planning: MR brain tumor segmentation and, volume measurement based on unsupervised fuzzy C-means clustering,’’ Int. J. Imag. Syst. Technol., vol. 25, no. 3, pp. 213–225, Sep. 2015, doi: 10.1002/ima.22139.
[9] J. Juan-Albarracín, E. Fuster-Garcia, J. V. Manjón, M. Robles, F. Aparici, L. Martí-Bonmatí, and J. M. García-Gómez, ‘‘Automated glioblastoma segmentation based on a multiparametric structured unsupervised classification,’’ PLoS ONE, vol. 10, no. 5, May 2015, Art. no. e0125143, doi: 10.1371/journal.pone.0125143.
[10] L. Rundo, C. Militello, A. Tangherloni, G. Russo, S. Vitabile, M. C. Gilardi, and G. Mauri, ‘‘NeXt for neuro-radiosurgery: A fully automatic approach for necrosis extraction in brain tumor MRI using an unsupervised machine learning technique,’’ Int. J. Imag. Syst. Technol., vol. 28, no. 1, pp. 21–37, Mar. 2018, doi: 10.1002/ima.22253.
[11] Y. Jiang, J. Hou, X. Xiao, and H. Deng, ‘‘A brain tumor segmentation new method based on statistical thresholding and multiscale CNN,’’ Intell. Comput. Methodologies, vol. 2, no. 3, pp. 235–245, 2019, doi: 10.1007/978-3-319-95957-3_26.
[12] D. Liu, D. Zhang, Y. Song, F. Zhang, L. J. O’Donnell, and W. Cai, ‘‘3D large kernel anisotropic network for brain tumor segmentation,’’ in Proc. Int. Conf. Neural Inf. Process. Cham, Switzerland: Springer, 2018 pp. 444–454, doi: 10.1007/978-3-030-04239-4_40.
[13] M. W. Nadeem, M. A. A. Ghamdi, M. Hussain, M. A. Khan, K. M. Khan, S. H. Almotiri, and S. A. Butt, ‘‘Brain tumor analysis empowered with deep learning: A review, taxonomy, and future challenges,’’ Brain Sci., vol. 10, no. 2, pp. 118–151, 2020, doi: 10.3390/brainsci10020118.
[14] Y. Bhanothu, A. Kamalakannan, and G. Rajamanickam, ‘‘Detection and classification of brain tumor in MRI images using deep convolutional network,’’ in Proc. 6th Int. Conf. Adv. Comput. Commun. Syst. (ICACCS), Mar. 2020, pp. 248–252, doi: 10.1109/ICACCS48705.2020.9074375.
[15] Z. Huang, X. Du, L. Chen, Y. Li, M. Liu, Y. Chou, and L. Jin, ‘‘Convolutional neural network based on complex networks for brain tumor image classification with a modified activation function,’’ IEEE Access, vol. 8, pp. 89281–89290, 2020, doi: 10.1109/ACCESS.2020.2993618.
[16] N. Abiwinanda, M. Hanif, S. T. Hesaputra, A. Handayani, and T. R. Mengko, ‘‘Brain tumor classification using convolutional neural network,’’ in Proc. World Congr. Med. Phys. Biomed. Eng., vol. 68, 2018, pp. 183–189, doi: 10.1007/978-981-10-9035-6_33.
[17] A. Ari and D. Hanbay, ‘‘Deep learning based brain tumor classification and detection system,’’ TURKISH J. Electr. Eng. Comput. Sci., vol. 26, no. 5, pp. 2275–2286, Sep. 2018, doi: 10.3906/elk-1801-8.
[18] Y. Ishikawa, K. Washiya, K. Aoki, and H. Nagahashi, ‘‘Brain tumor classification of microscopy images using deep residual learning,’’ in Proc. SPIE, vol. 10013, 2016, Art. no. 100132Y, doi: 10.1117/12.2242711.

[19] H. Mohsen, E.-S. A. El-Dahshan, E.-S. M. El-Horbaty, and A.-B. M. Salem, ‘‘Classification using deep learning neural networks for brain tumors,’’ Future Comput. Informat. J., vol. 3, no. 1, pp. 68–71, 2018, doi: 10.1016/j.fcij.2017.12.001.
[20] J. S. Paul, A. J. Plassard, B. A. Landman, and D. Fabbri, ‘‘Deep learning for brain tumor classification,’’ in Proc. SPIE, vol. 10137, 2017, pp. 1013710–1013726, doi: 10.1117/12.2254195.
[21] Y. Xu, Z. Jia, Y. Ai, F. Zhang, M. Lai, and E. I-Chao Chang, ‘‘Deep convolutional activation features for large scale brain tumor histopathology image classification and segmentation,’’ in Proc. IEEE Int. Conf. Acoust., Speech Signal Process. (ICASSP), South Brisbane, QLD, Australia, Apr. 2015, pp. 947–951, doi: 10.1109/ICASSP.2015. 7178109.
[22] K. B. Ahmed, L. O. Hall, D. B. Goldgof, R. Liu, and R. A. Gatenby, ‘‘Fine-tuning convolutional deep features for MRI based brain tumor classification,’’ in Proc.
[23] M. R. Ismael, ‘‘Hybrid model—Statistical features and deep neural network for brain tumor classification in MRI images,’’ Ph.D. dissertation, Western Michigan Univ., Kalamazoo, MI, USA, 2018. [Online]. Available: https://scholarworks.wmich.edu/dissertations/3291
[24] R. Liu, L. O. Hall, D. B. Goldgof, M. Zhou, R. A. Gatenby, and K. B. Ahmed, ‘‘Exploring deep features from brain tumor magnetic resonance images via transfer learning,’’ in Proc. Int. Joint Conf. Neural Netw. (IJCNN), Jul. 2016, pp. 235–242, doi: 10.1109/IJCNN.2016.7727204.
[25] C. N. Ladefoged, L. Marner, A. Hindsholm, I. Law, L. Højgaard, and F. L. Andersen, ‘‘Deep learning-based attenuation correction of PET/MRI in pediatric brain tumor patients: Evaluation in a clinical setting,’’ Frontiers Neurosci, vol. 2, p. 1005, Jan. 2018, doi: 10.3389/fnins.2018.01005.
[26] H. Fabelo, M. Halicek, S. Ortega, M. Shahedi, A. Szolna, J. Piñeiro, C. Sosa, A. O’Shanahan, S. Bisshopp, C. Espino, M. Márquez, M. Hernández, D. Carrera, J. Morera, G. Callico, R. Sarmiento, and B. Fei, ‘‘Deep learning-based framework for in vivo identification of glioblastoma tumor using hyperspectral images of human brain,’’ Sensors, vol. 19, no. 4, p. 920, Feb. 2019, doi: 10.3390/s19040920.
[27] Y. Li and L. Shen, ‘‘Deep learning based multimodal brain tumor diagnosis,’’ in Proc. Int. MICCAI Brainlesion Workshop, vol. 10670, 2017, pp. 149–158, doi: 10.1007/978-3-319-75238-9_13.
[28] L. Chato and S. Latifi, ‘‘Machine learning and deep learning techniques to predict overall survival of brain tumor patients using MRI images,’’ in Proc. IEEE 17th Int. Conf. Bioinf. Bioengineering (BIBE), Oct. 2017, pp. 9–14, doi: 10.1109/BIBE.2017.00-86.
[29] B. Amarapur, ‘‘Computer-aided diagnosis applied to MRI images of brain tumor using cognition based modified level set and optimized ANN classifier,’’ Multimedia Tools Appl., vol. 3601, pp. 3571–3599, Feb. 2020, doi: 10.1007/s11042-018-6308-7.
[30] E. Benson, M. P. Pound, A. P. French, A. S. Jackson, and T. P. Pridmore, ‘‘Deep hourglass for brain tumor segmentation,’’ in Proc. Int. MICCAI Brainlesion Workshop, vol. 10, no. 2, 2018, pp. 419–428, doi: 10.3390/brainsci10020118.
[31] C. Zhou, S. Chen, C. Ding, and D. Tao, ‘‘Learning contextual and attentive information for brain tumor segmentation,’’ in Proc. Int. MICCAI Brainlesion Workshop, vol. 4798, 2018, pp. 497–507, doi: 10.1007/978-3-030-11726-9_44.

[32] G. Kim, ‘‘Brain tumor segmentation using deep fully convolutional neural networks,’’ in Brainlesion: Glioma, Multiple Sclerosis, Stroke and Traumatic Brain Injuries (Lecture Notes in Computer Science), vol. 10670, A. Crimi, S. Bakas, H. Kuijf, B. Menze, and M. Reyes, Eds. Cham, Switzerland: Springer, 2018, doi: 10.1007/978-3-319-75238- 9_30.
[33] P. Afshar, A. Mohammadi, and K. N. Plataniotis, ‘‘Brain tumor type classification via capsule networks,’’ in Proc. 25th IEEE Int. Conf. Image Process. (ICIP), Oct. 2018, pp. 3129–3133, doi: 10.1109/ICIP.2018.8451379.
[34] P. D. Chang, ‘‘Fully convolutional deep residual neural networks for brain tumor segmentation,’’ in Proc. Int. Workshop Brainlesion, 2016, pp. 108–118, doi: 10.1007/978-3-319-55524-9_11.
[35] F. Isensee et al., ‘‘Brain tumor segmentation using large receptive field deep convolutional neural networks,’’ in Bildverarbeitung für die Medizin 2017 (Informatik aktuell), K. H. Maier-Hein, geb. Fritzsche, T. M. Deserno, geb. Lehmann, H. Handels, and T. Tolxdorff, Eds. Berlin, Germany: Springer Vieweg, 2017, doi: 10.1007/978-3-662-54345- 0_24.
[36] S. Kumar, A. Negi, and J. N. Singh, ‘‘Semantic segmentation using deep learning for brain tumor MRI via fully convolution neural networks,’’ in Information and Communication Technology for Intelligent Systems. Singapore: Springer, 2019, pp. 11–19, doi: 10.1007/978-981-13-1742- 2_2.
[37] A. M. Hasan, H. A. Jalab, F. Meziane, H. Kahtan, and A. S. Al-Ahmad, ‘‘Combining deep and handcrafted image features for MRI brain scan classification,’’ IEEE Access, vol. 7, pp. 79959–79967, 2019, doi: 10.1109/ACCESS.2019.2922691.
[38] S. Deepak and P. M. Ameer, ‘‘Brain tumor classification using deep CNN features via transfer learning,’’ Comput. Biol. Med., vol. 111, pp. 1–7, Aug. 2019, doi: 10.1016/j.compbiomed.2019.103345. [39] H. M. Rai and K. Chatterjee, ‘‘2D MRI image analysis and brain tumor detection using deep learning CNN model LeU-Net,’’ Multimedia Tools Appl., vol. 80, nos. 28–29, pp. 36111–36141, Nov. 2021, doi: 10.1007/s11042-021-11504-9.
[40] V. K. Deepak and R. Sarath, ‘‘An intelligent brain tumor segmentation using improved deep learning model based on cascade regression method,’’ Multimedia Tools Appl., pp. 1–20, Dec. 2022, doi: 10.1007/s11042-022-13945-2.
[41] E. U. Haq, H. Jianjun, K. Li, H. U. Haq, and T. Zhang, ‘‘An MRI-based deep learning approach for efficient classification of brain tumors,’’ J. Ambient Intell. Humanized Comput., pp. 1–22, Oct. 2021, doi: 10.1007/s12652-021-03535-9.
[42] S. Sajid, S. Hussain, and A. Sarwar, ‘‘Brain tumor detection and segmentation in MR images using deep learning,’’ Arabian J. Sci. Eng., vol. 44, no. 11, pp. 9249–9261, Nov. 2019, doi: 10.1007/s13369-019-03967-8.
[43] R. Ranjbarzadeh, A. B. Kasgari, S. J. Ghoushchi, S. Anari, M. Naseri, and M. Bendechache, ‘‘Brain tumor segmentation based on deep learning and an attention mechanism using MRI multi-modalities brain images,’’ Sci. Rep., vol. 11, no. 1, p. 10930, May 2021, doi: 10.1038/s41598-021-90428-8.
[44] T. Ruba, R. Tamilselvi, and M. P. Beham, ‘‘Brain tumor segmentation in multimodal MRI images using novel LSIS operator and deep learning,’’ J. Ambient Intell. Humanized Comput., pp. 1–15, Mar. 2022, doi: 10.1007/s12652-022-03773-5.

[45] A. Verma and V. P. Singh, ‘‘Design, analysis and implementation of efficient deep learning frameworks for brain tumor classification,’’ Multimedia Tools Appl., vol. 81, no. 26, pp. 37541–37567, Nov. 2022, doi: 10.1007/s11042-022-13545-0.
[46] P. K. Ramtekkar, A. Pandey, and M. K. Pawar, ‘‘Innovative brain tumor detection using optimized deep learning techniques,’’ Int. J. Syst. Assurance Eng. Manage., vol. 14, no. 1, pp. 459–473, Feb. 2022, doi: 10.1007/s13198-022-01819-7.
[47] R. Rajasree, C. C. Columbus, and C. Shilaja, ‘‘Multiscale-based multimodal image classification of brain tumor using deep learning method,’’ Neural Comput. Appl., vol. 33, no. 11, pp. 5543–5553, Jun. 2021, doi: 10.1007/s00521-020-05332-5.
[48] M. A. H. Tuhin, T. Pramanick, H. K. Emon, W. Rahman, M. M. I. Rahi, and M. A. Alam, ‘‘Detection and 3D visualization of brain tumor using deep learning and polynomial interpolation,’’ in Proc. IEEE Asia– Pacific Conf. Comput. Sci. Data Eng. (CSDE), Dec. 2020, pp. 1–6, doi: 10.1109/CSDE50874.2020.9411595.
[49] R. D. Shirwaikar, K. Ramesh, and A. Hiremath, ‘‘A survey on brain tumor detection using machine learning,’’ in Proc. Int. Conf. Forensics, Analytics, Big Data, Secur. (FABS), vol. 1, Dec. 2021, pp. 1–6, doi: 10.1109/FABS52071.2021.9702583.
[50] H. Yahyaoui, F. Ghazouani, and I. R. Farah, ‘‘Deep learning guided by an ontology for medical images classification using a multimodal fusion,’’ in Proc. Int. Congr. Adv. Technol. Eng. (ICOTEN), 2021, pp. 1–6, doi: 10.1109/ICOTEN52080.2021.9493469.
[51] S. Pokhrel, L. K. Dahal, N. Gupta, R. Shrestha, A. Srivastava, and A. Bhasney, ‘‘Brain tumor detection application based on convolutional neural network,’’ in Proc. 2nd Int. Conf. Intell. Technol. (CONIT), Jun. 2022, pp. 1–5, doi: 10.1109/CONIT55038.2022.9848177.
[52] S. Gull, S. Akbar, and K. Safdar, ‘‘An interactive deep learning approach for brain tumor detection through 3D-magnetic resonance images,’’ in Proc. Int. Conf. Frontiers Inf. Technol. (FIT), Dec. 2021, pp. 114–119, doi: 10.1109/FIT53504.2021.00030.
[53] Y. Suter, A. Jungo, M. Rebsamen, U. Knecht, E. Herrmann, R. Wiest, and M. Reyes, ‘‘Deep learning versus classical regression for brain tumor patient survival prediction,’’ in Proc. Int. MICCAI Brainlesion Workshop, 2019, pp. 429–440, doi: 10.1007/978-3-030-11726-9_38.
[54] Y. Hu and Y. Xia, ‘‘3D deep neural network-based brain tumor segmentation using multimodality magnetic resonance sequences,’’ in Proc. Int. MICCAI Brainlesion Workshop, 2017, pp. 423–434, doi: 10.1007/978-3-319-75238-9_36.
[55] D. Nie, H. Zhang, E. Adeli, L. Liu, and D. Shen, ‘‘3D deep learning for multi-modal imaging-guided survival time prediction of brain tumor patients,’’ in Proc. Int. Conf. Med. Image Comput. Comput.-Assist. Intervent., 2016, pp. 212–220, doi: 10.1007/978-3-319-46723-8_25.
[56] G. Anand Kumar and P. V. Sridevi, ‘‘3D deep learning for automatic brain MR tumor segmentation with T-spline intensity inhomogeneity correction,’’ Autom. Control Comput. Sci., vol. 52, no. 5, pp. 439–450, Sep. 2018, doi: 10.3103/S0146411618050048.
[57] G. Chetty, M. Yamin, and M. White, ‘‘A low resource 3D U-Net based deep learning model for medical image analysis,’’ Int. J. Inf. Technol., vol. 14, no. 1, pp. 95–103, Feb. 2022, doi: 10.1007/s41870-021- 00850.

[58] Z. Shaukat, Q. U. A. Farooq, S. Tu, C. Xiao, and S. Ali, ‘‘A state-ofthe-art technique to perform cloud-based semantic segmentation using deep learning 3D U-Net architecture,’’ BMC Bioinf., vol. 23, no. 1, pp. 251–272, Dec. 2022, doi: 10.1186/s12859-022-04794-9.
[59] H. Mzoughi, I. Njeh, A. Wali, M. B. Slima, A. BenHamida, C. Mhiri, and K. B. Mahfoudhe, ‘‘Deep multi-scale 3D convolutional neural network (CNN) for MRI gliomas brain tumor classification,’’ J. Digit. Imag., vol. 33, no. 4, pp. 903–915, Aug. 2020, doi: 10.1007/ s10278-020-00347-9.
[60] J. N. Stember and H. Shalu, ‘‘Deep reinforcement learning with automated label extraction from clinical reports accurately classifies 3D MRI brain volumes,’’ J. Digit. Imag., vol. 35, no. 5, pp. 1143–1152, Oct. 2022, doi: 10.1007/s10278-022-00644-5.
[61] Y. Jun, T. Eo, T. Kim, H. Shin, D. Hwang, S. H. Bae, Y. W. Park, H. J. Lee, B. W. Choi, and S. S. Ahn, ‘‘Deep-learned 3D black-blood imaging using automatic labelling technique and 3D convolutional neural networks for detecting metastatic brain tumors,’’ Sci. Rep., vol. 8, pp. 9450–9461, 2018, doi: 10.1038/s41598-018-27742-1.
[62] P. Agrawal, N. Katal, and N. Hooda, ‘‘Segmentation and classification of brain tumor using 3D-UNet deep neural networks,’’ Int. J. Cognit. Comput. Eng., vol. 3, pp. 199–210, Jun. 2022, doi: 10.1016/ j.ijcce.2022.11.001.
[63] A. S. Akbar, C. Fatichah, and N. Suciati, ‘‘Single level UNet3D with multipath residual attention block for brain tumor segmentation,’’ J. King Saud Univ. Comput. Inf. Sci., vol. 34, no. 6, pp. 3247–3258, Jun. 2022, doi: 10.1016/j.jksuci.2022.03.022.
[64] H. T. Zaw, ‘‘Brain tumor detection based on Naïve Bayes classification,’’ in Proc. 5th Int. Conf. Eng., Appl. Sci. Technol. (ICEAST), 2019, pp. 1–4, doi: 10.1109/ICEAST.2019.8802562.
[65] E. Sert, F. Özyurt, and A. Dogantekin, ‘‘A new approach for brain tumor diagnosis system: Single image super-resolution based maximum fuzzy entropy segmentation and convolutional neural network,’’ Med. Hypothesis, vol. 133, pp. 1–9, Dec. 2019, doi: 10.1016/ j.mehy.2019.109413.
[66] T. L. Narayana and T. S. Reddy, ‘‘An efficient optimization technique to detect brain tumor from MRI images,’’ in Proc. Int. Conf. Smart Syst. Inventive Technol., 2018, pp. 1–4, doi: 10.1109/ICSSIT.2018. 8748288.
[67] F. P. Polly, S. K. Shil, M. A. Hossain, A. Ayman, and Y. M. Jang, ‘‘Detection and classification of HGG and LGG brain tumor using machine learning,’’ in Proc. Int. Conf. Inf. Netw. (ICOIN), Jan. 2018, pp. 813–817, doi: 10.1109/ICOIN.2018.8343231.
[68] J. Amin, M. Sharif, M. Yasmin, and S. L. Fernandes, ‘‘A distinctive approach in brain tumor detection and classification using MRI,’’ Pattern Recognit. Lett., vol. 139, pp. 1–10, Nov. 2017, doi: 10.1016/j.patrec.2017.10.036.
[69] N. Gupta and P. Khanna, ‘‘A non-invasive and adaptive CAD system to detect brain tumor from T2-weighted MRIs using customized Otsu’s thresholding with prominent features and supervised learning,’’ Signal Process., Image Commun., vol. 59, pp. 18–26, Nov. 2017, doi: 10.1016/j.image.2017.05.013.
[70] N. Gupta, P. Bhatele, and P. Khanna, ‘‘Identification of Gliomas from brain MRI through adaptive segmentation and run length of centralized patterns,’’ J. Comput. Sci., vol. 25, pp. 1–8, Mar. 2017, doi: 10.1016/j.jocs.2017.02.009.

[71] A. Minz and C. Mahobiya, ‘‘MR image classification using Adaboost for brain tumor type,’’ in Proc. Int. Advance Comput. Conf., 2017, pp. 1–5, doi: 10.1109/IACC.2017.0146.
[72] A. S. Shankar, A. Asokan, and D. Sivakumar, ‘‘Brain tumor classification using Gustafson–Kessel (G-k) fuzzy clustering algorithm,’’ Int. J. Latest Eng. Res. Appl., vol. 1, pp. 68–72, Aug. 2016.
[73] M. K. Islam, M. S. Ali, M. S. Miah, M. M. Rahman, M. S. Alam, and M. A. Hossain, ‘‘Brain tumor detection in MR image using superpixels, principal component analysis and template based K-means clustering algorithm,’’ Mach. Learn. Appl., vol. 5, Sep. 2021, Art. no. 100044, doi: 10.1016/j.mlwa.2021.100044.
[74] S. Banerjee, S. Mitra, F. Masulli, and S. Rovetta, ‘‘Deep radiomics for brain tumor detection and classification from multi-sequence MRI,’’ Social Netw. Comput. Sci., vol. 1, no. 4, pp. 1–15, 2019, doi: 10.1007/s42979-020-00214-y.
[75] A. Naseer, T. Yasir, A. Azhar, T. Shakeel, and K. Zafar, ‘‘Computer-aided brain tumor diagnosis: Performance evaluation of deep learner CNN using augmented brain MRI,’’ Int. J. Biom.Imag., vol. 2021, pp. 1–11, Jun. 2021, doi: 10.1155/2021/5513500.
[76] I. Abd El Kader, G. Xu, Z. Shuai, S. Saminu, I. Javaid, I. S. Ahmad, and S. Kamhi, ‘‘Brain tumor detection and classification on MR images by a deep wavelet auto-encoder model,’’ Diagnostics, vol. 11, no. 9, p. 1589, Aug. 2021, doi: 10.3390/diagnostics11091589.
[77] L. Sheeba, A. Mitra, S. Chaudhuri, and S. D. Sarkar, ‘‘Detection of exact location of brain tumor from MRI data using big data analytics,’’ Systematic Rev. Pharmacy, vol. 12, no. 5, pp. 378–381, 2021, doi: 10.5530/srp.2020.1.01.
[78] J. Amin, M. Sharif, A. Haldorai, M. Yasmin, and R. S. Nayak, ‘‘Brain tumor detection and classification using machine learning: A comprehensive survey,’’ Complex Intell. Syst., vol. 8, pp. 3163–3183, Nov. 2022, doi: 10.1007/s40747-021-00563-y.
[79] M. Shahajad, D. Gambhir, and R. Gandhi, ‘‘Features extraction for classification of brain tumor MRI images using support vector machine,’’ in Proc. 11th Int. Conf. Cloud Comput., Data Sci. Eng. (Confluence), 2021, pp. 767–772, doi: 10.1109/Confluence51648.2021.9377111.
[80] E. Alberts, G. Tetteh, S. Trebeschi, M. Bieth, A. Valentinitsch, B. Wiestler, C. Zimmer, and B. H. Menze, ‘‘Multi-modal image classification using low-dimensional texture features for genomic brain tumor recognition,’’ in Proc. Int. Workshop Graphs Biomed. Image Anal., vol. 10551, pp. 201–209, 2017, doi: 10.1007/978-3-319-67675-3_18.